

Primordial magnetic field signals in the 21 cm background

Kerstin Kunze

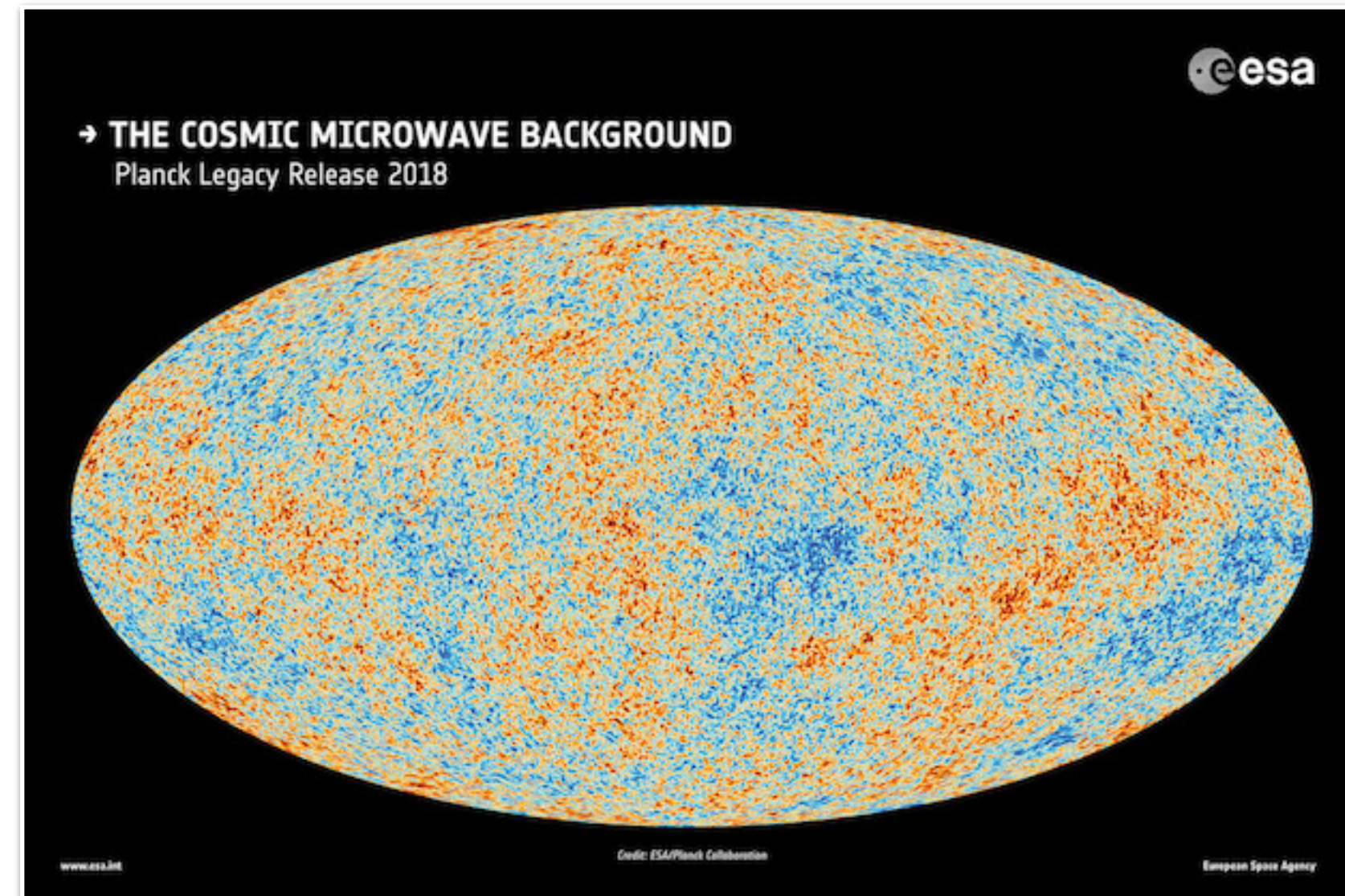
(Universidad de Salamanca)

Overview

- Modelling cosmological magnetic fields and effects
- Effects on the matter power spectrum
- Simulations: modified matter density field induced 21 cm line signal
- Observations
- Conclusions

Modelling cosmological magnetic fields

- Global isotropy rules out significant homogeneous magnetic field.



Modelling cosmological magnetic fields

Assumptions

- Origin of magnetic fields in the very early universe
- Stochastic magnetic field

Most general form:
helical magnetic field

Consider only non
helical magnetic
field.

$$\langle B_i^*(\vec{k}) B_j(\vec{q}) \rangle = \delta_{\vec{k}, \vec{q}} \mathcal{P}_S(k) \left(\delta_{ij} - \frac{k_i k_j}{k^2} \right) + \delta_{\vec{k}, \vec{k}'} P_A(k) i \epsilon_{ijm} \hat{k}_m$$

where

$$\mathcal{P}_M(k, k_m, k_L) = A_M \left(\frac{k}{k_L} \right)^{n_M} W(k, k_m)$$

$M = S, A$ pivot scale

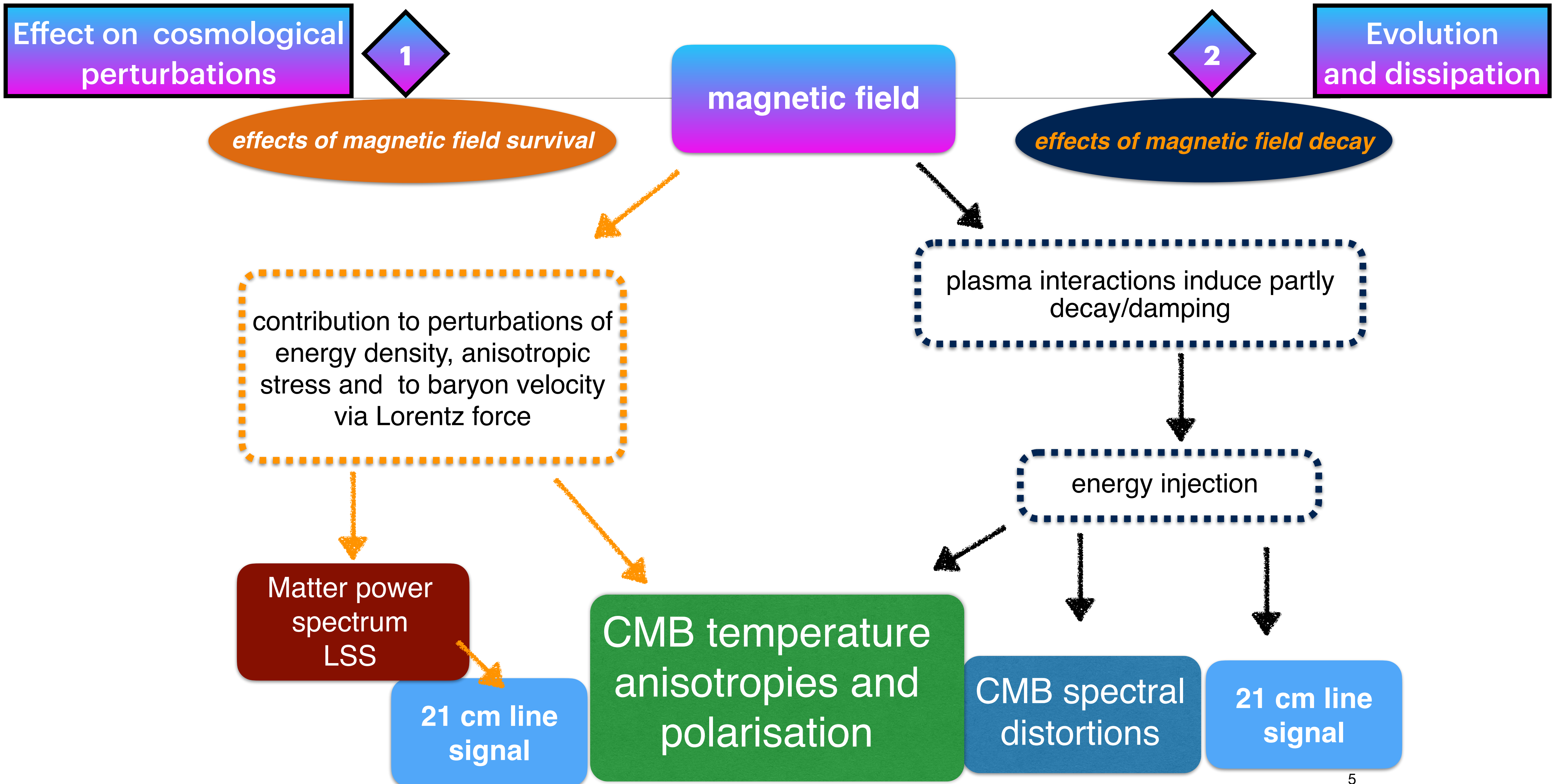
window function

$$W(k, k_m) = \pi^{-\frac{3}{2}} k_m^{-3} e^{-(k/k_m)^2}$$

damping scale

upper cut-off

Evolution and observational effects



Dissipation of cosmic magnetic fields: How and Where to

Damping of magnetic fields

There is also damping around neutrino decoupling at around $z \sim 10^{10}$ when a black body spectrum is always restored. (no spectral distortions)

○ Before decoupling of photons

▶ viscous damping

■ After decoupling of photons

▶ decaying MHD turbulence

▶ ambipolar diffusion



energy injection



change in thermal and ionisation history

radiative viscosity

$z > z_{dec}$

decaying MHD turbulence

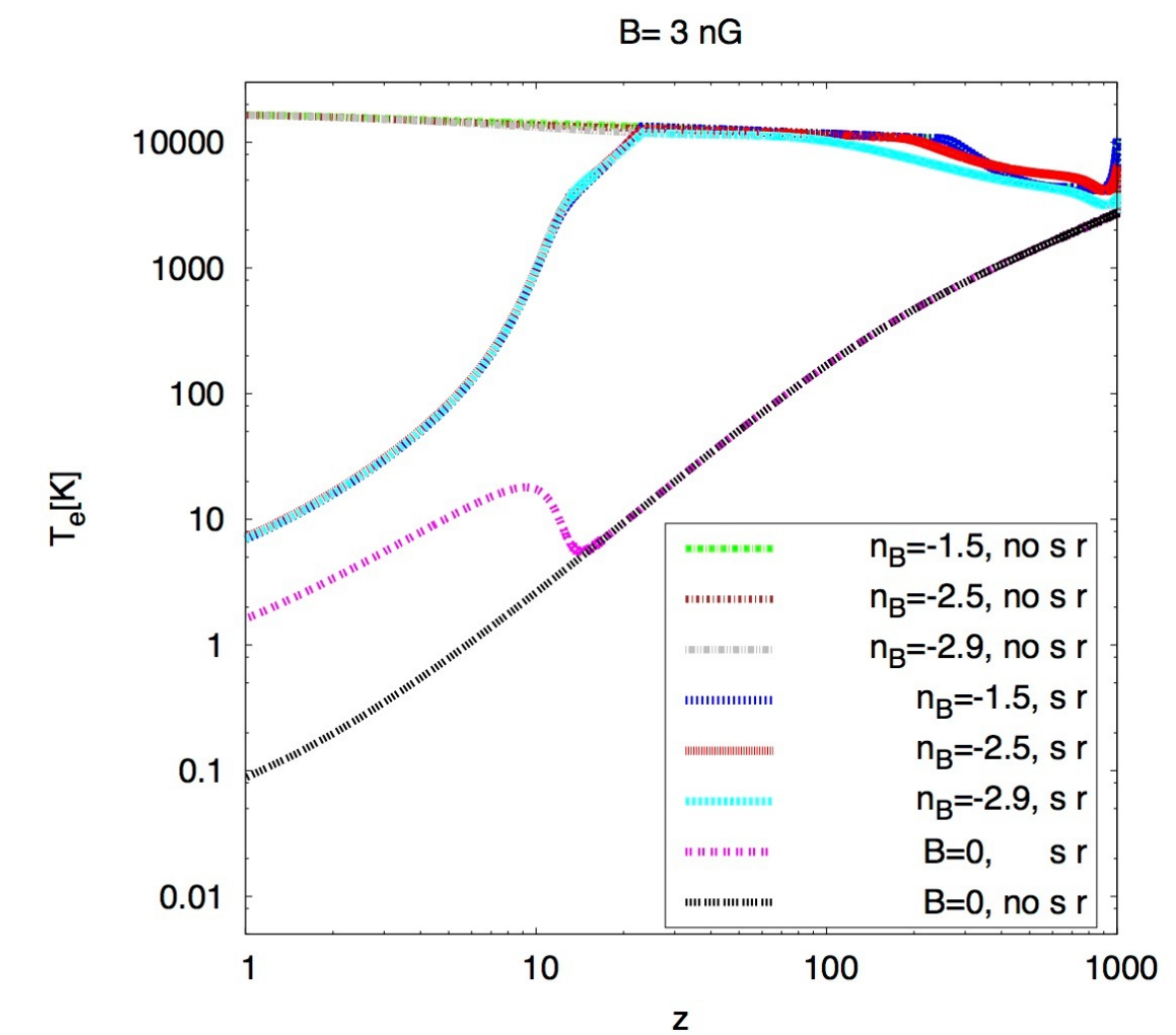
$z_{dec} > z > 100$

ambipolar diffusion

$z < 100$

Evolution of electron temperature

$$\dot{T}_e = -2\frac{\dot{a}}{a}T_e + \frac{x_e}{1+x_e} \frac{8\rho_\gamma\sigma_T}{3m_e c} (T_\gamma - T_e) + \frac{x_e\Gamma}{1.5k_B n_e}$$



Effect of magnetic mode on the linear matter power spectrum and 21cm line signal

- Total linear matter power spectrum: primordial curvature mode + magnetic mode

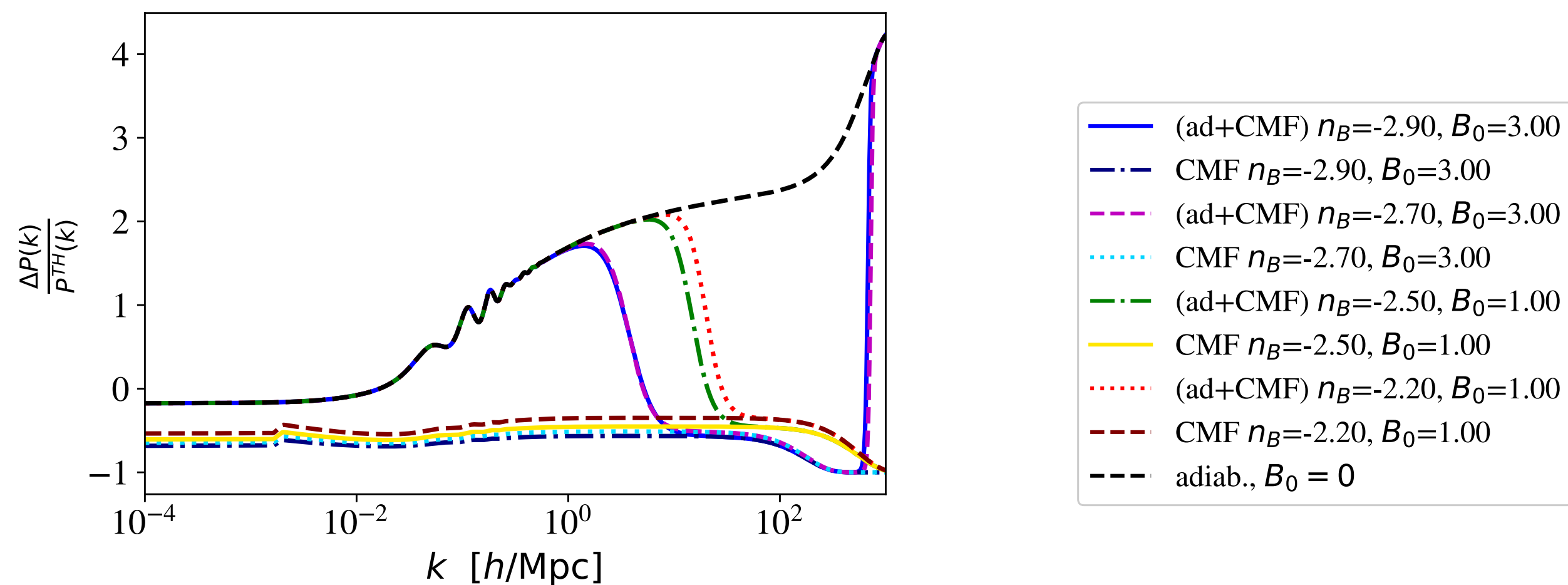
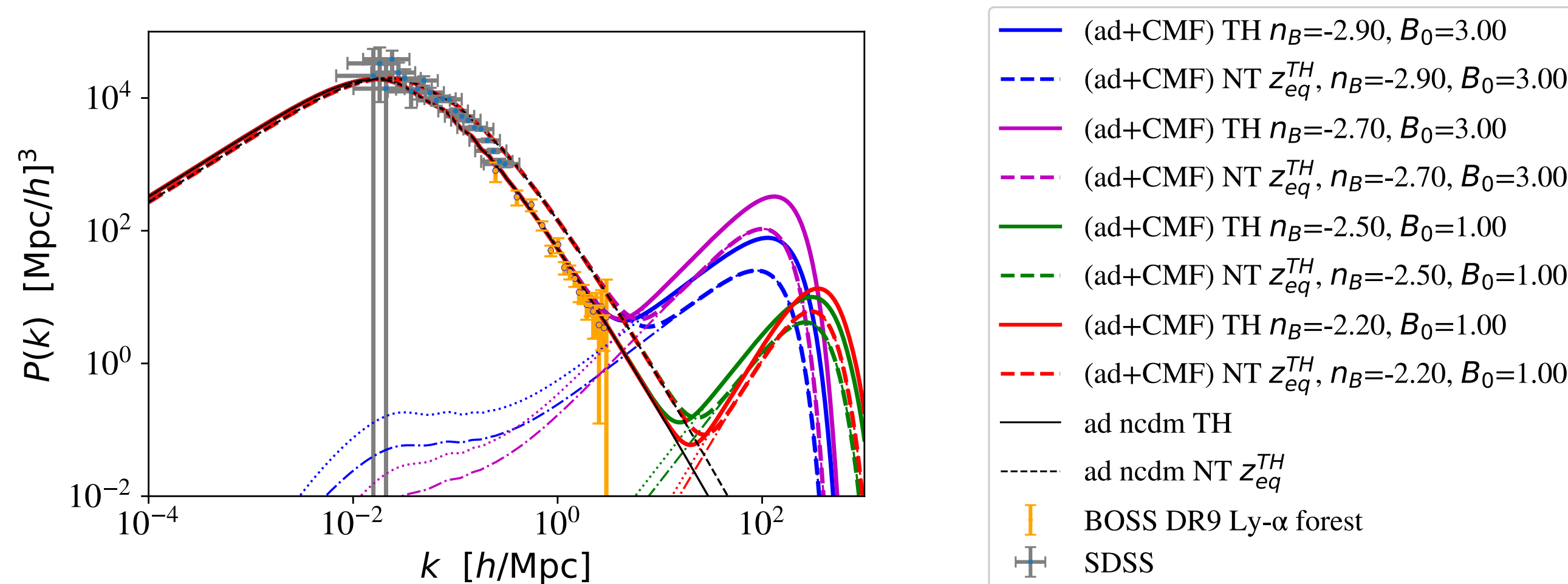
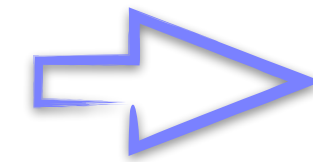


Figure 7. Linear matter power spectrum for three thermal neutrinos (TH) and three non-thermal neutrinos (NT, z_{eq}^{TH}) with distribution function (2.1) for different choices of the magnetic field parameters (B_0 [nG], n_B). *Upper panel:* the total linear matter power spectrum of the adiabatic mode (ad) and the compensated magnetic mode (CMF) is shown together with data points from BOSS DR9 Ly- α forrest [42] and SDSS [43]. The light dotted and dashed-dotted lines indicate the three neutrino thermal magnetic mode and the three neutrino non-thermal pure magnetic mode solutions, respectively. z_{eq}^{TH} denotes that the cosmological parameters have been adjusted so that the redshift of radiation-matter equality in the non-thermal model is the same as that in the non-thermal one (see details in the text). *Lower panel:* relative change of the linear matter power spectrum w.r.t. to the three thermal neutrino model (TH).

Effect of magnetic mode on the linear matter power spectrum and 21cm line signal

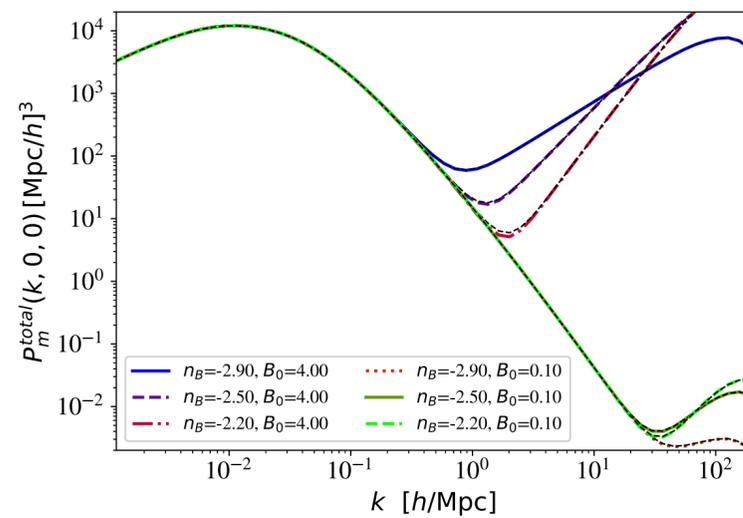
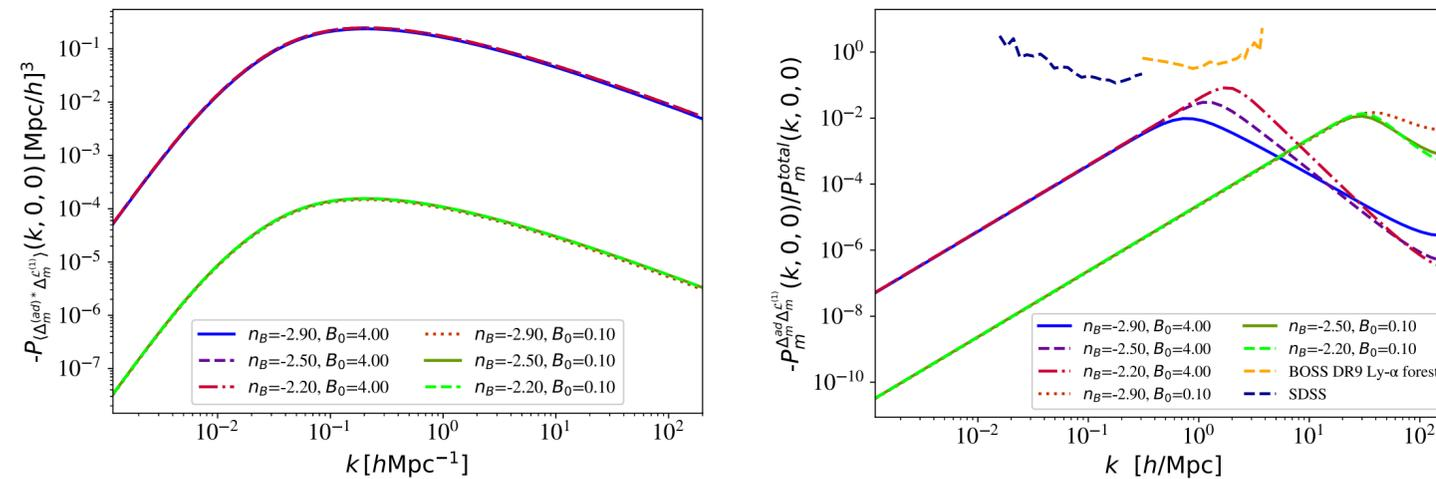
Beyond the frozen-in approximation of the comoving magnetic field



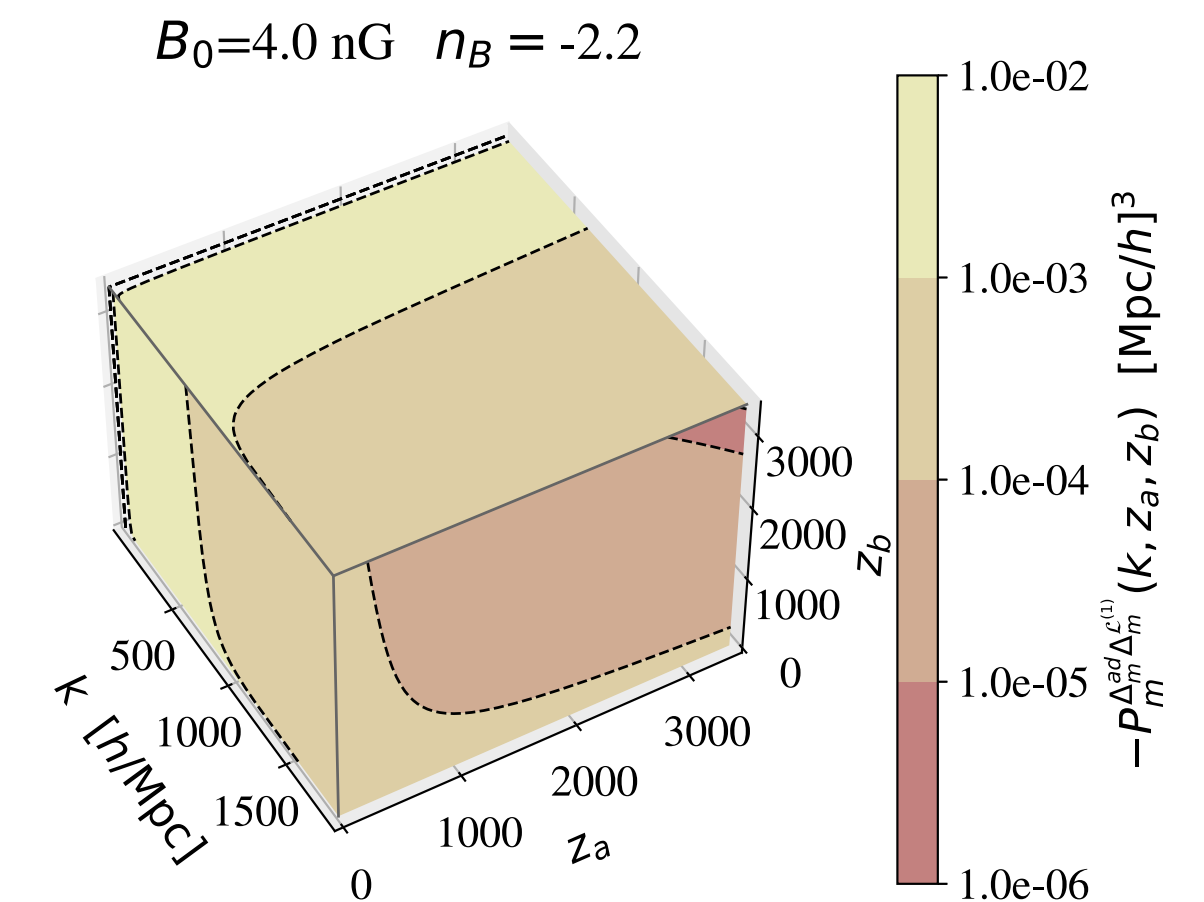
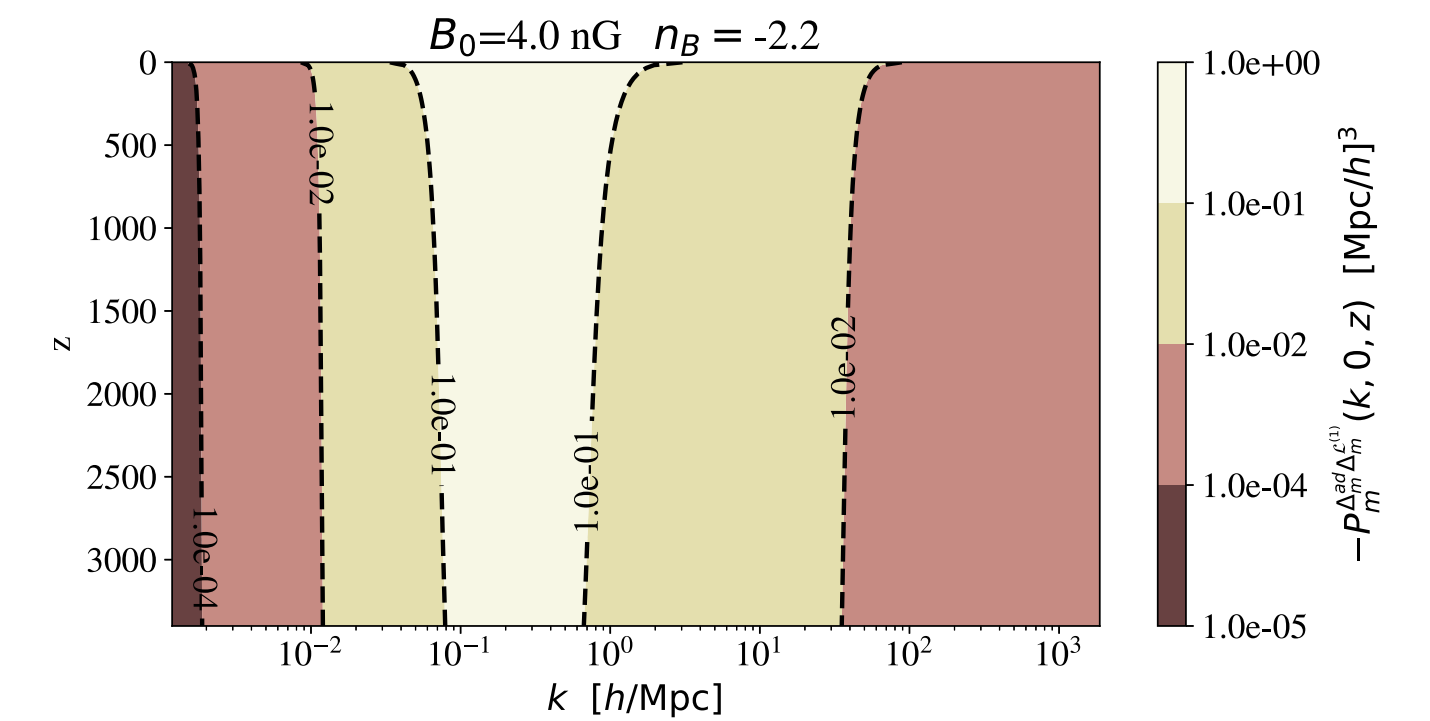
cross correlation between primordial curvature and magnetic mode induced matter density perturbations

Unequal time (redshift) cross correlation spectral functions at present

Equal time cross correlation spectral functions at present

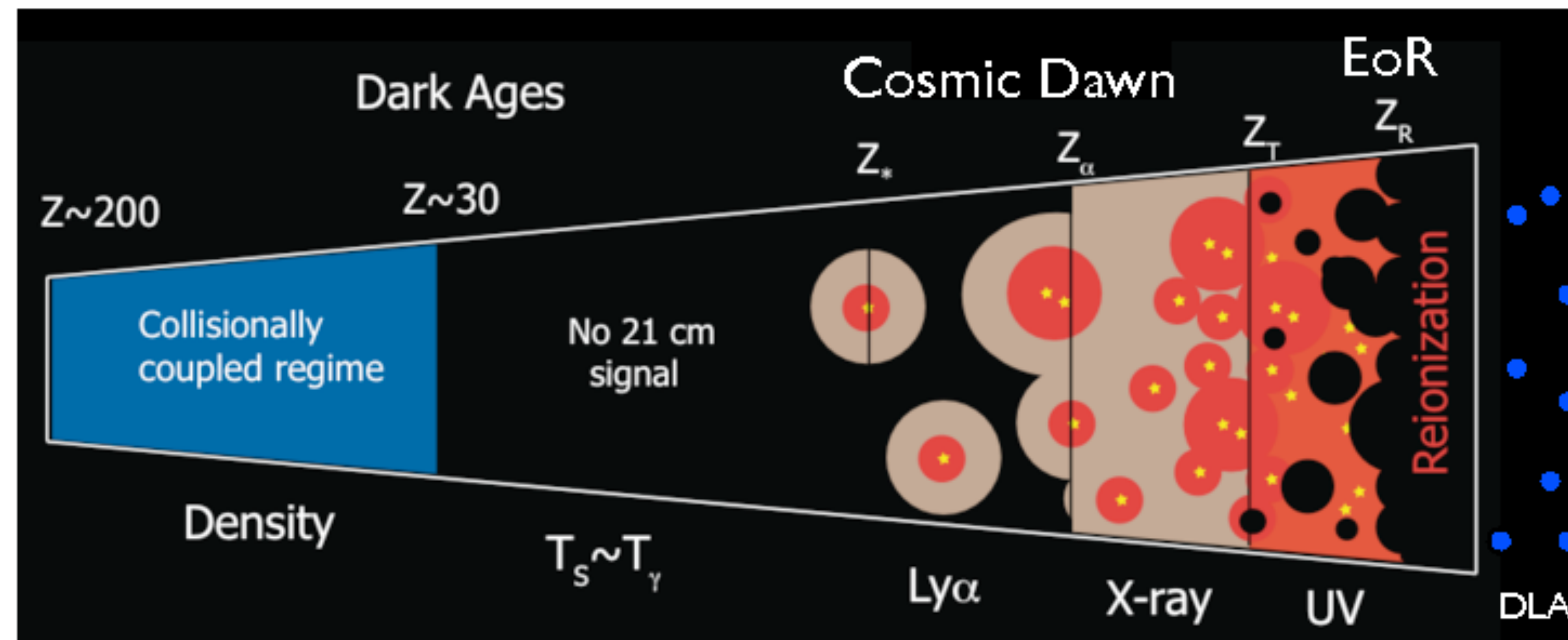


Total matter power spectrum including cross correlation at present



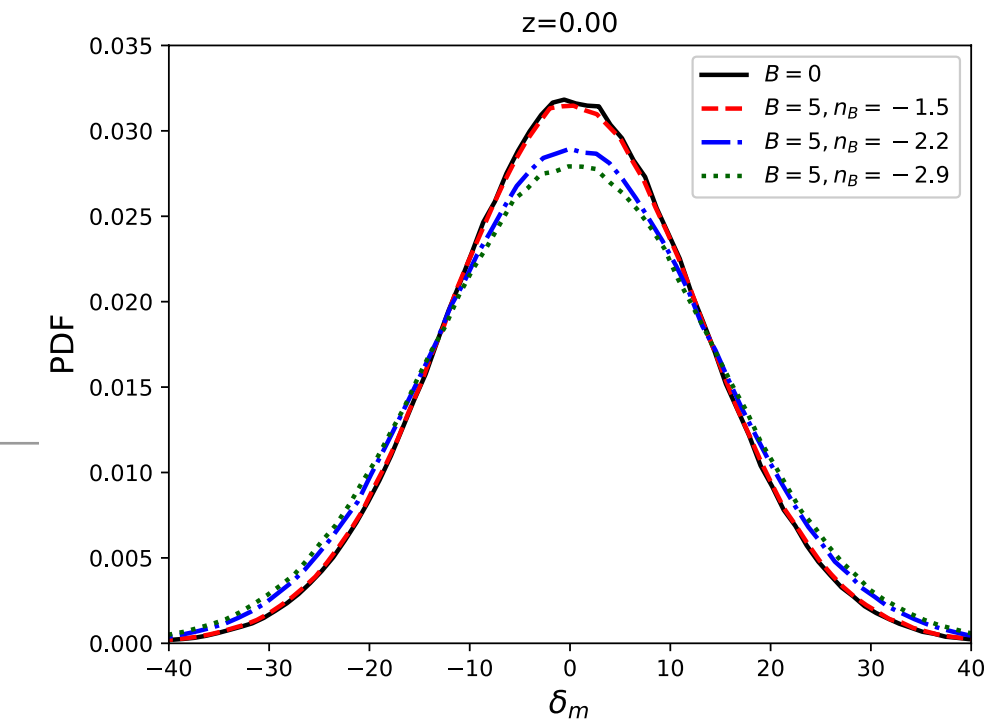
Effect of magnetic mode on the linear matter power spectrum and 21 cm line signal

21 cm line signal: change in brightness temperature of CMB due to hyperfine transition in neutral hydrogen atoms along line of sight

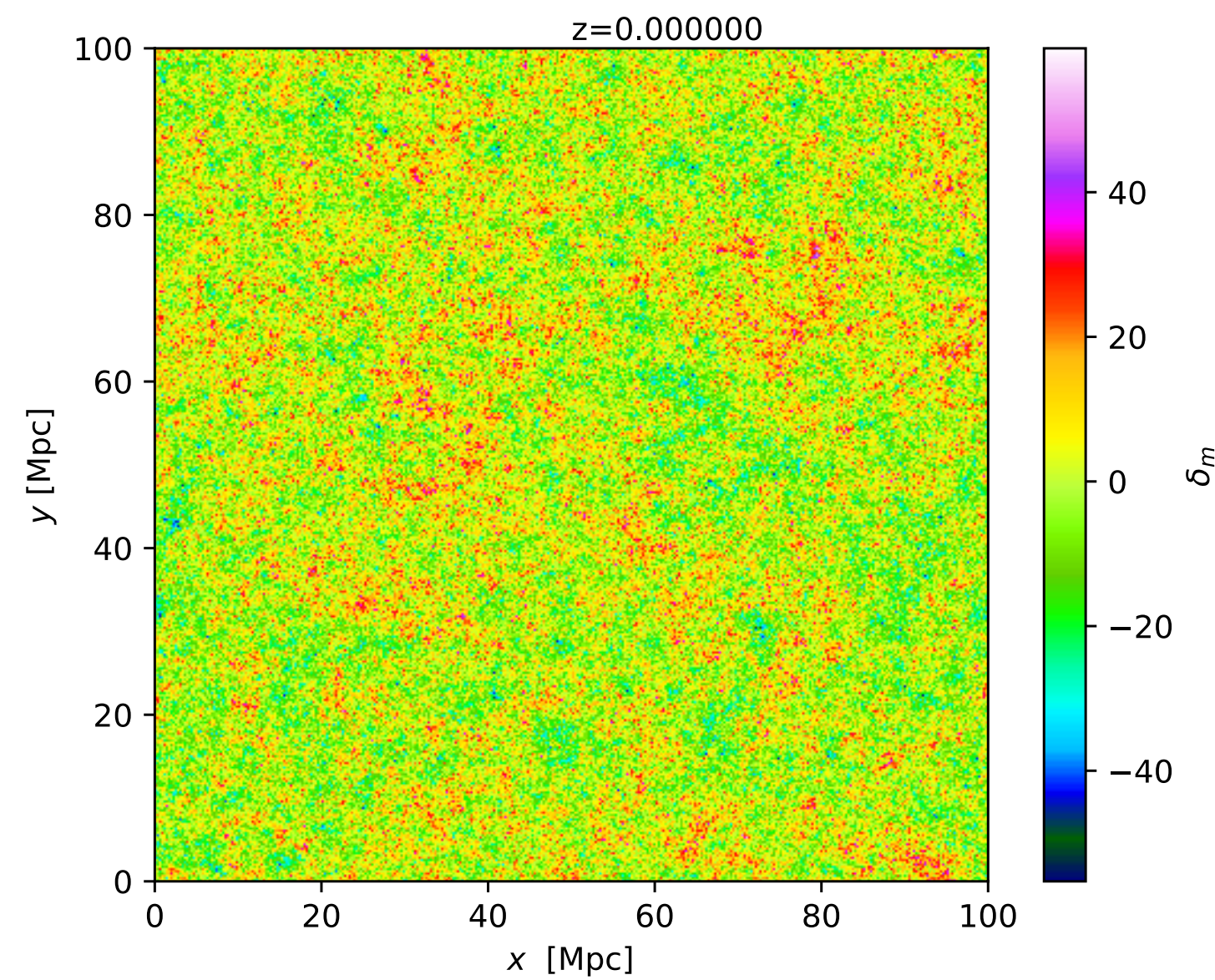


Simulations: matter density field

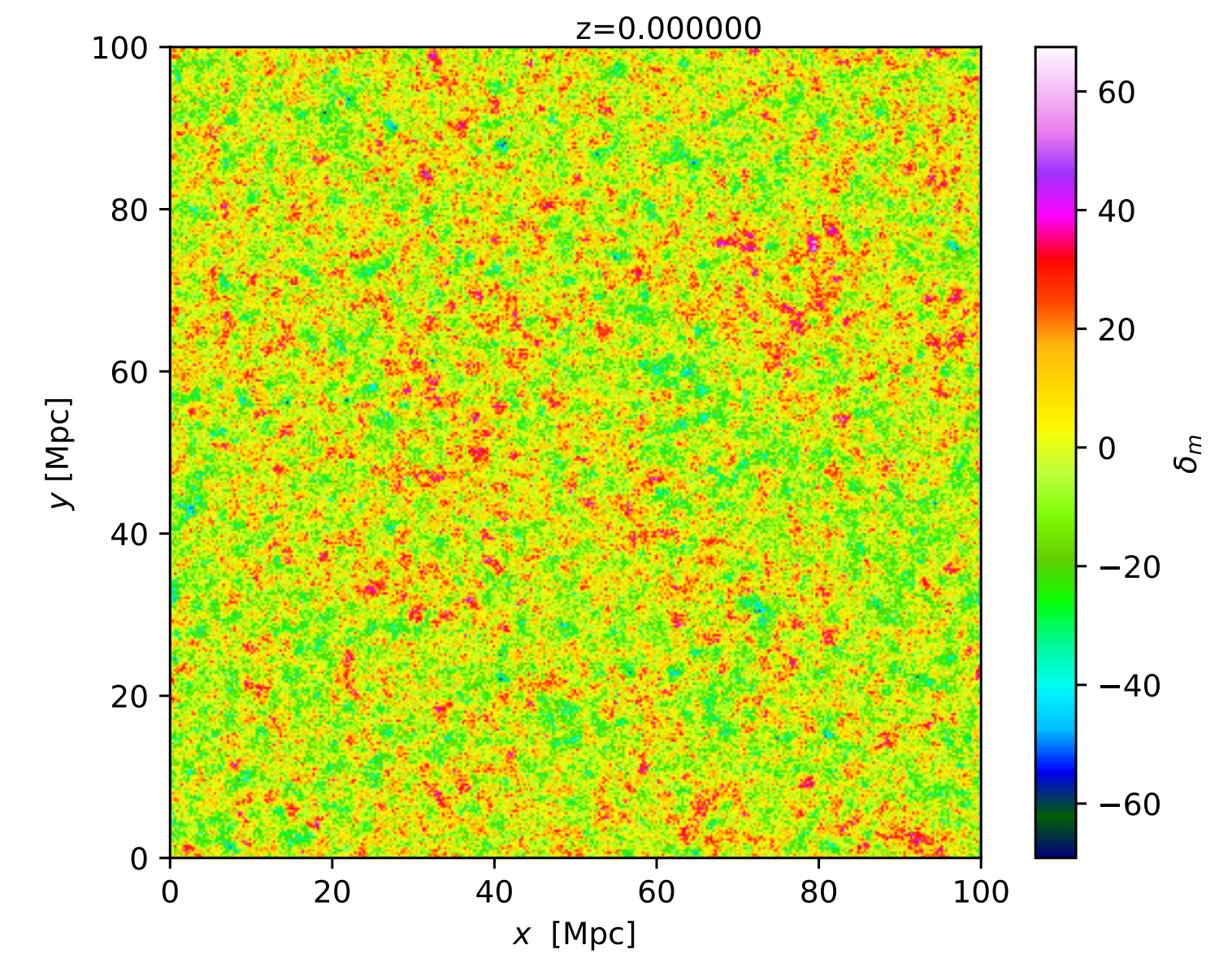
- Linear density matter field



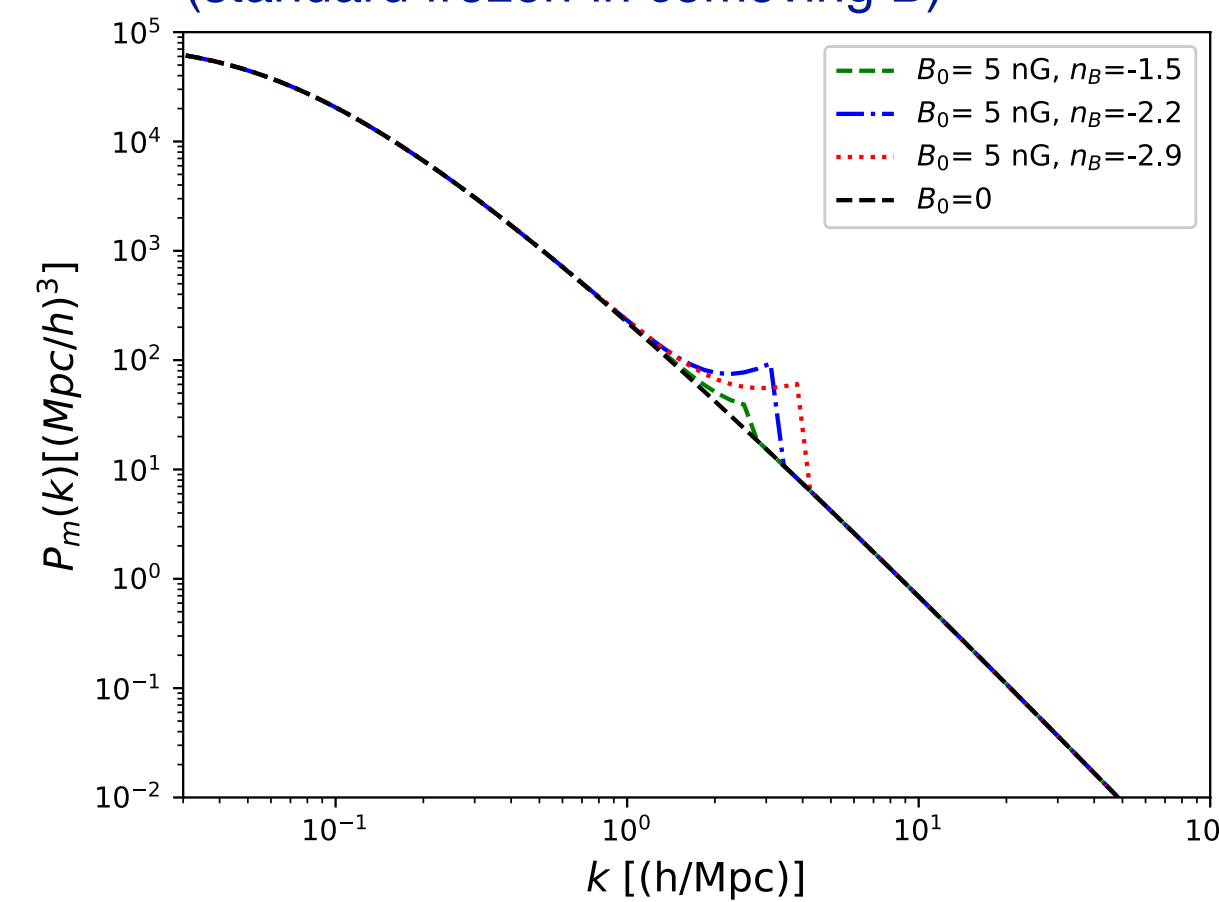
B=0



B=5 nG, $n_B=-2.9$



Initial total linear matter power spectrum: primordial curvature mode + magnetic mode (standard frozen-in comoving B)



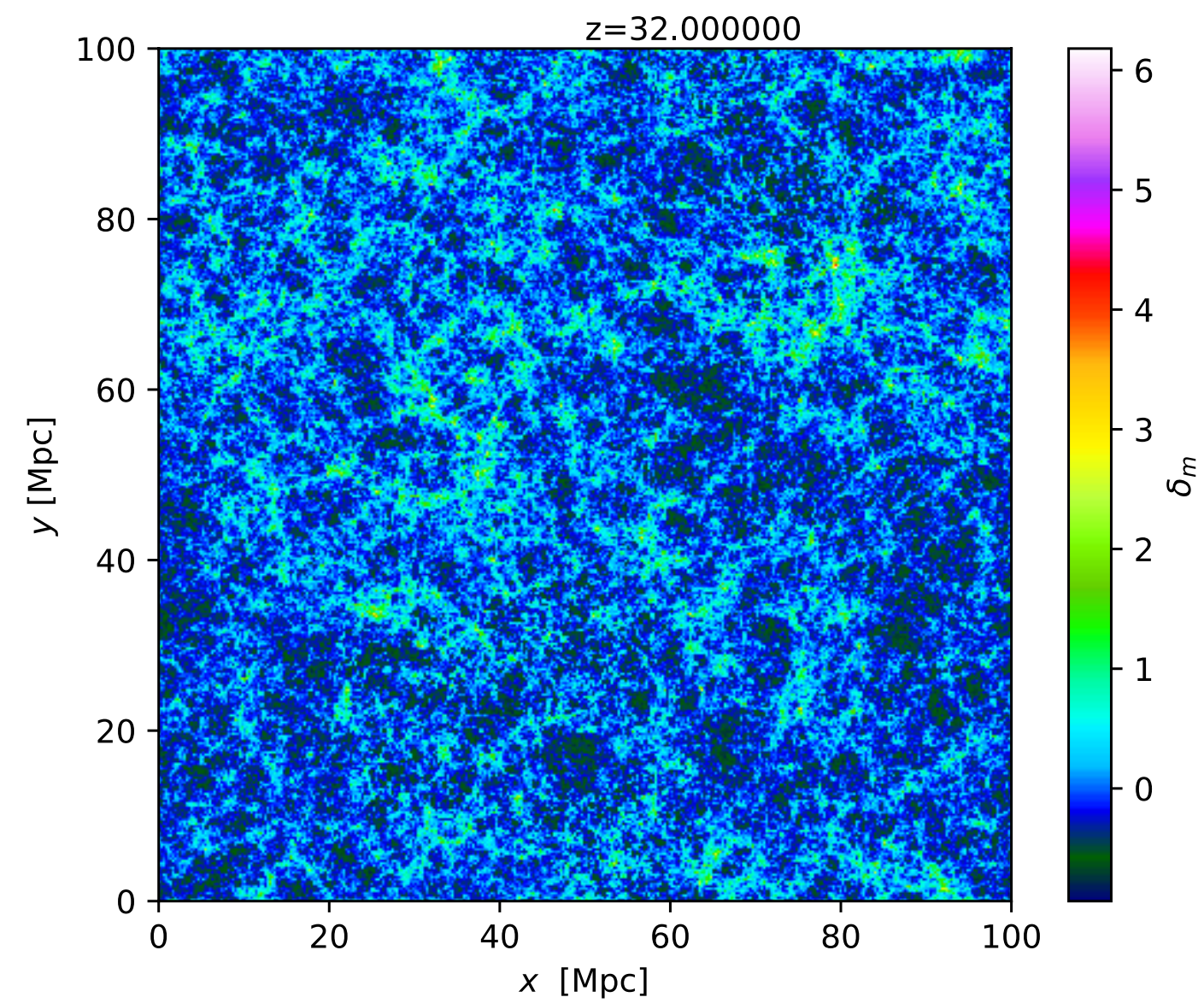
Simulations with modified version of Simfast21 (Santos et al.)

KK 2019

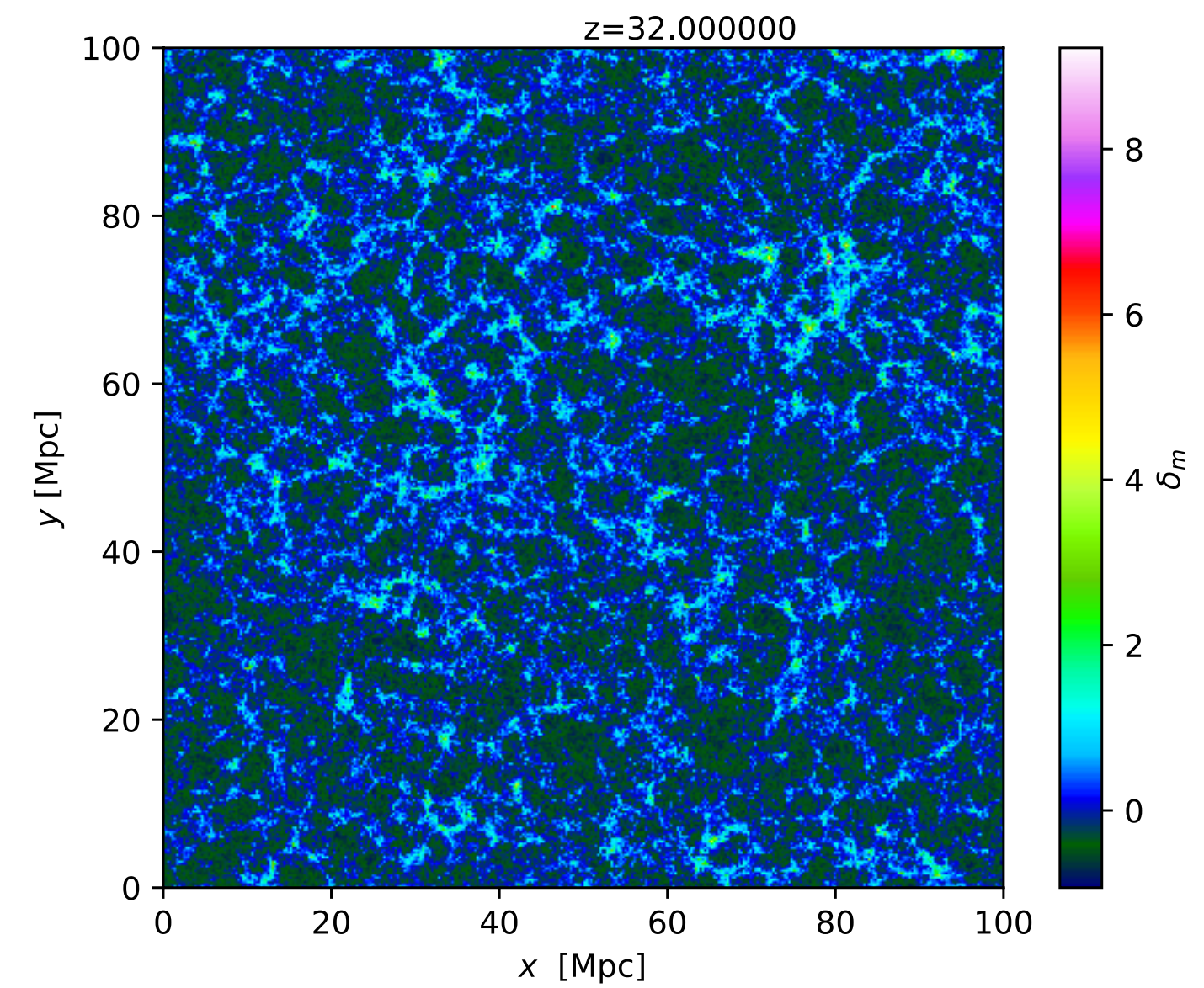
Simulations: matter density field

- non linear density matter field **z=32**

B=5 nG, nB=-1.5



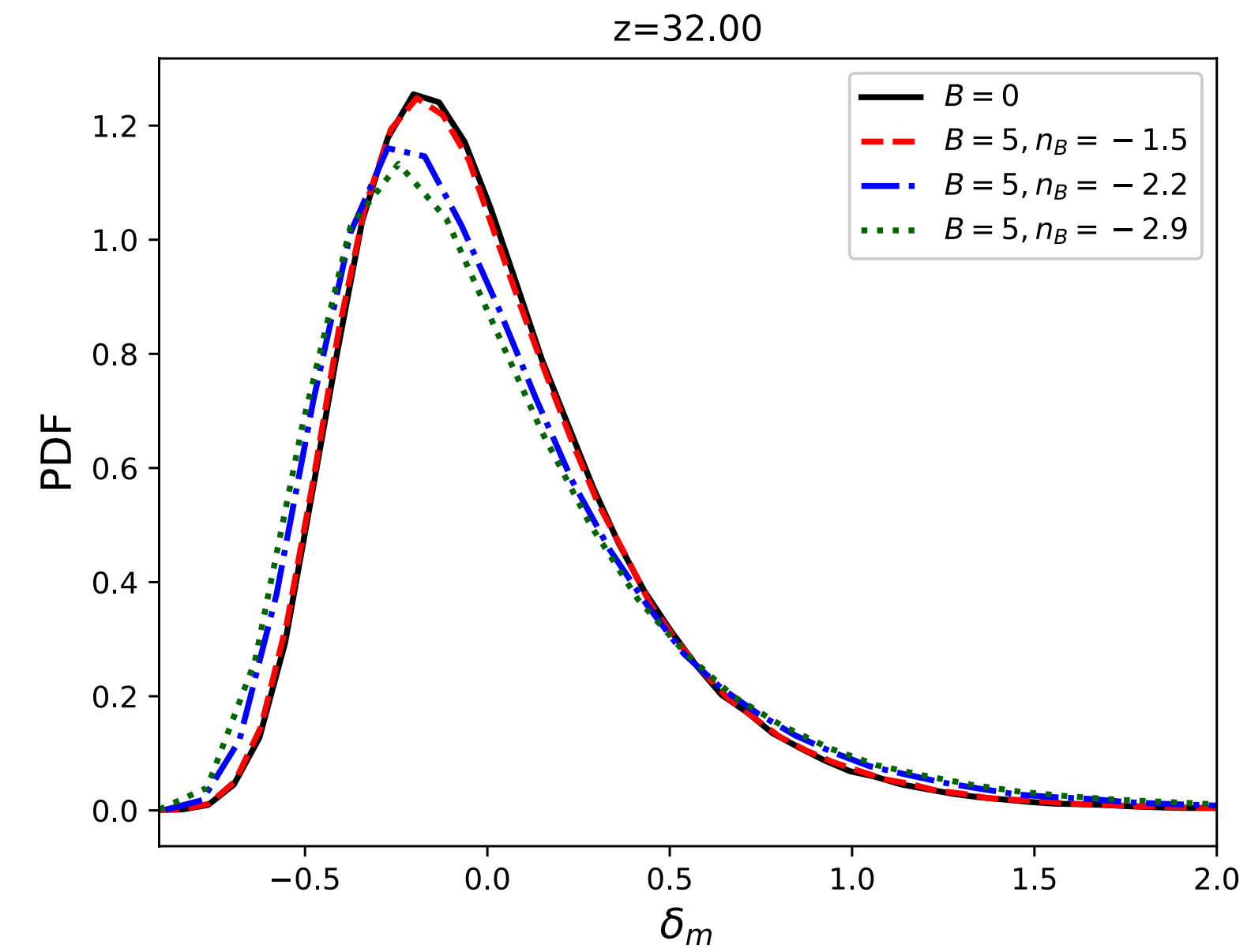
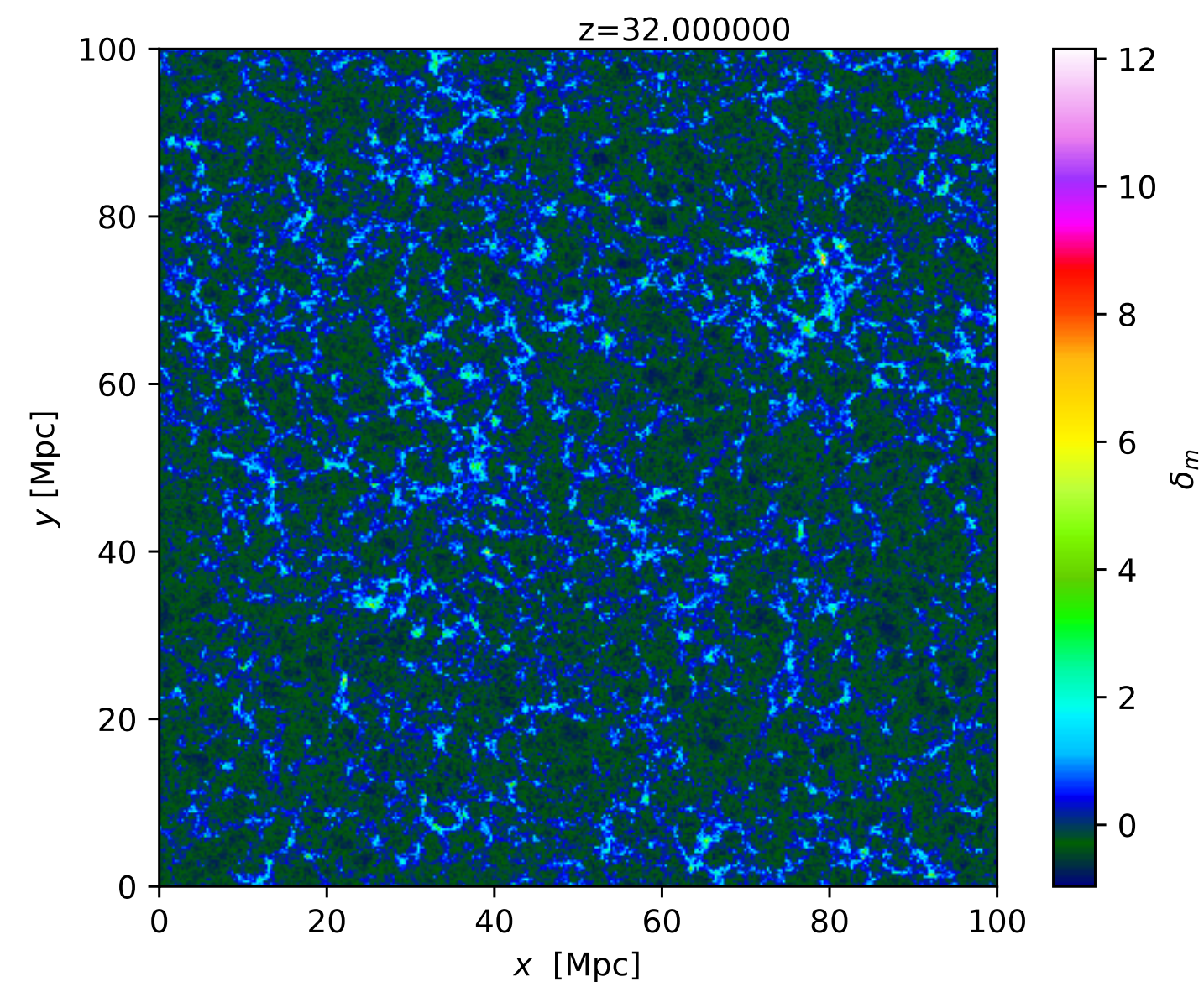
B=5 nG, nB=-2.2



Simulations: matter density field

- non linear density matter field **z=32**

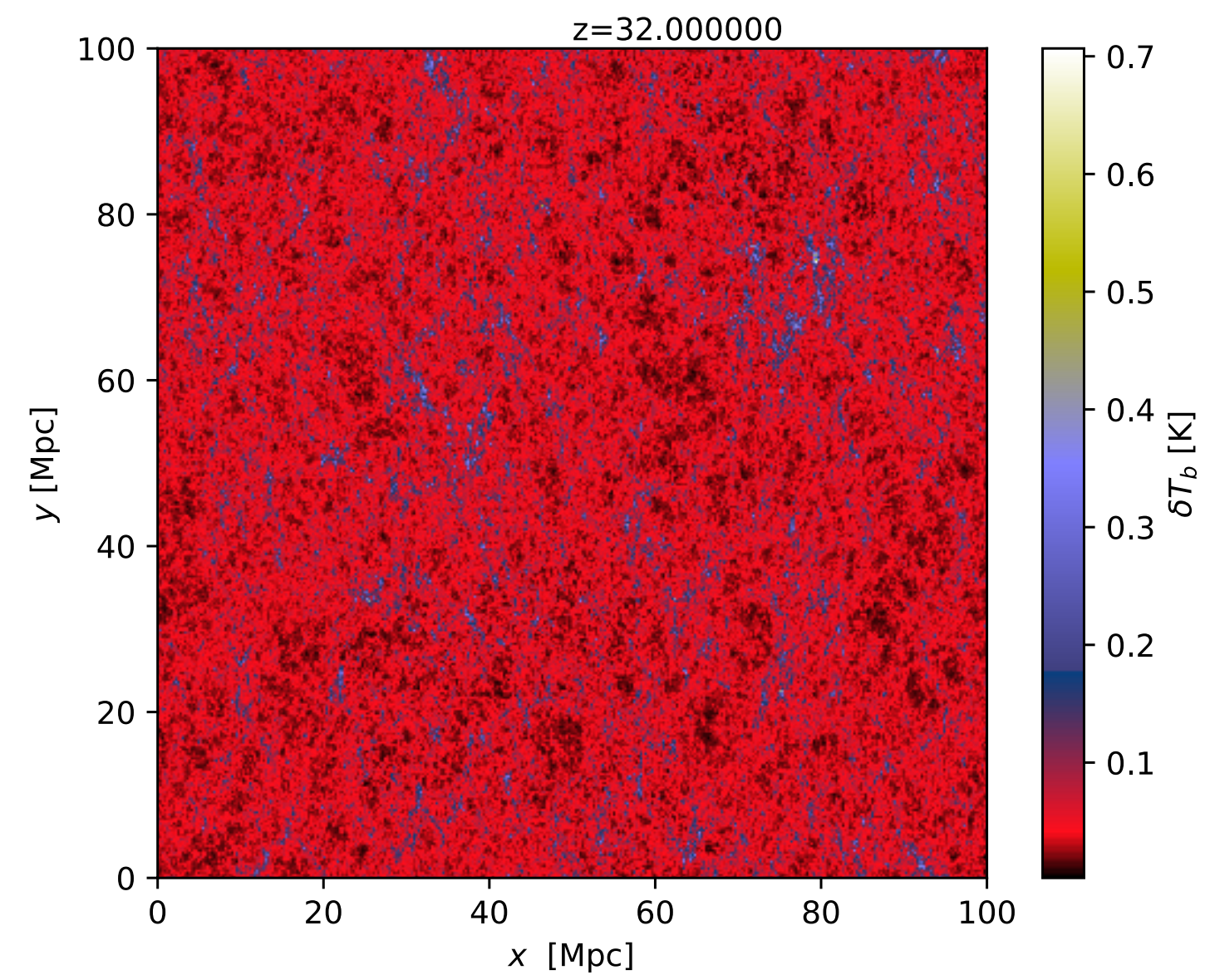
B=5 nG, nB=-2.9



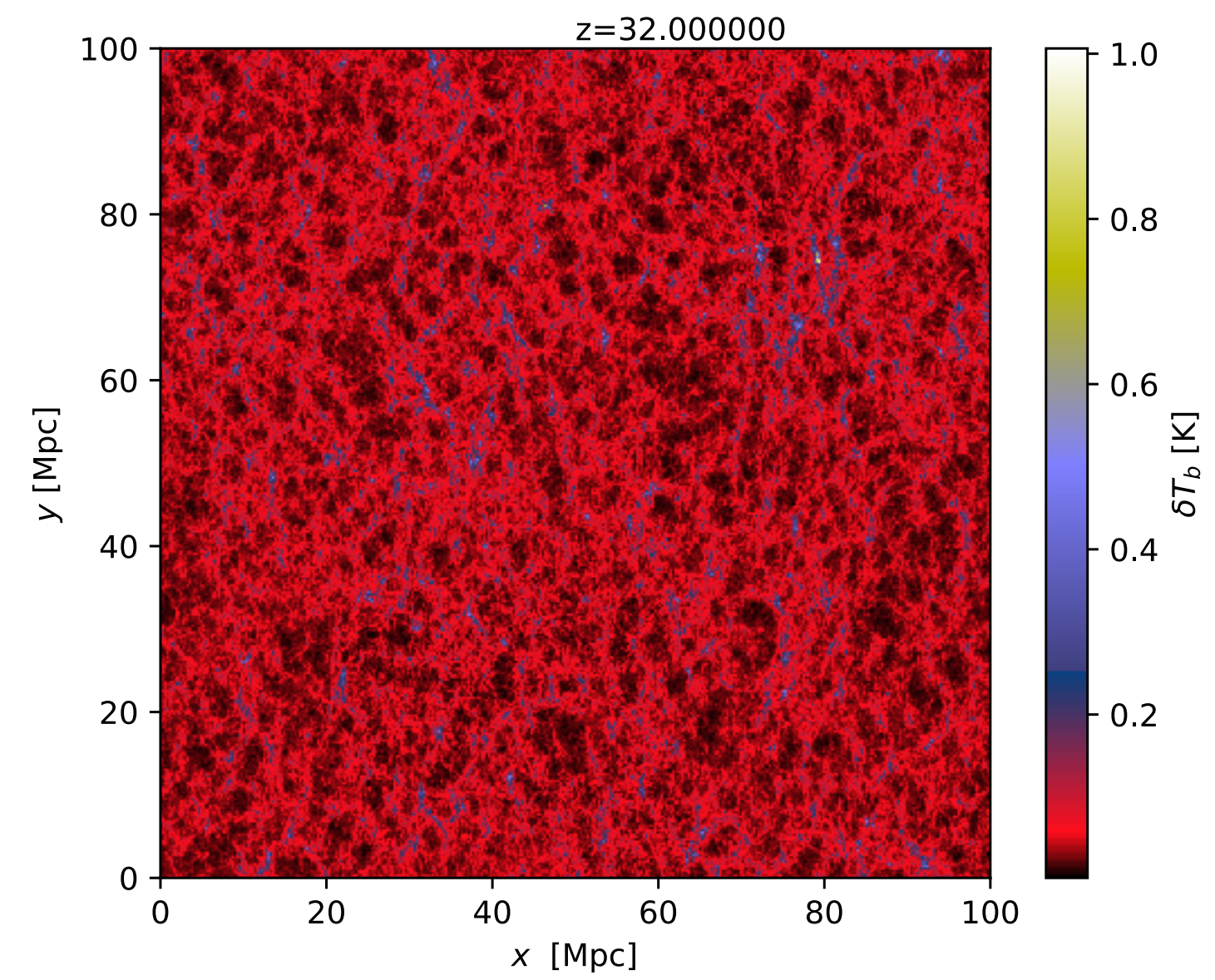
Simulations: 21 cm line signal

z=32

B=5 nG, nB=-1.5



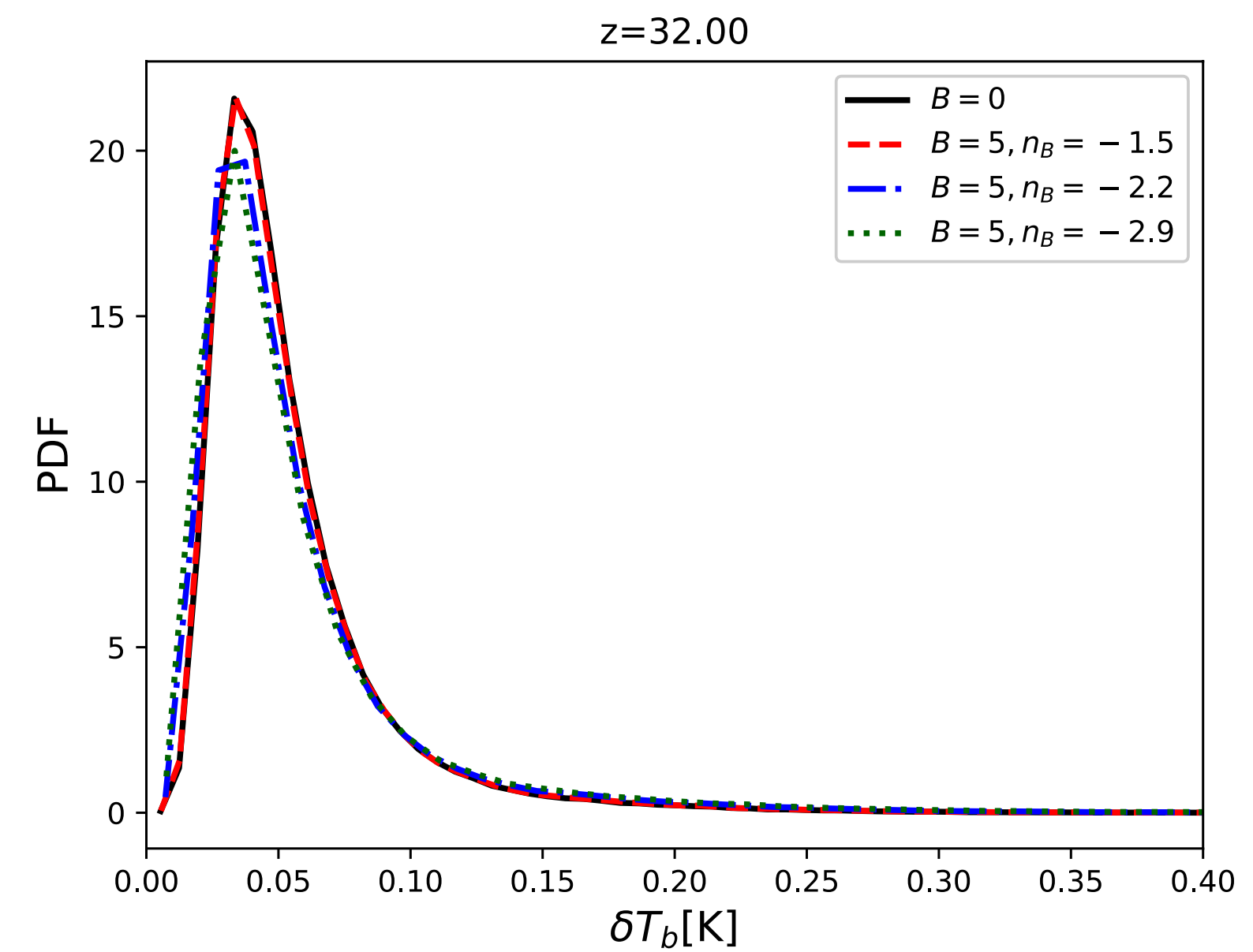
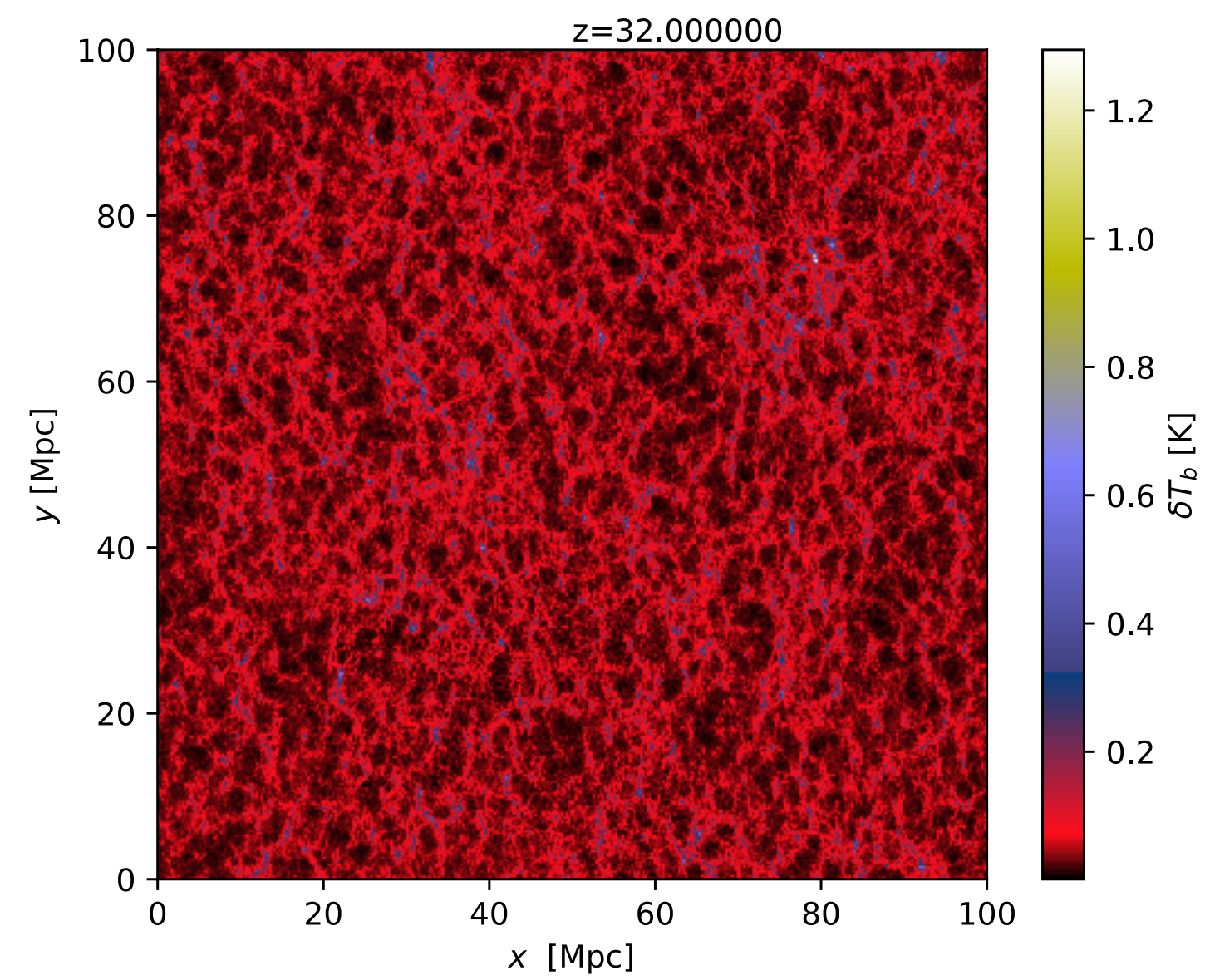
B=5 nG, nB=-2.2



Simulations: 21 cm line signal

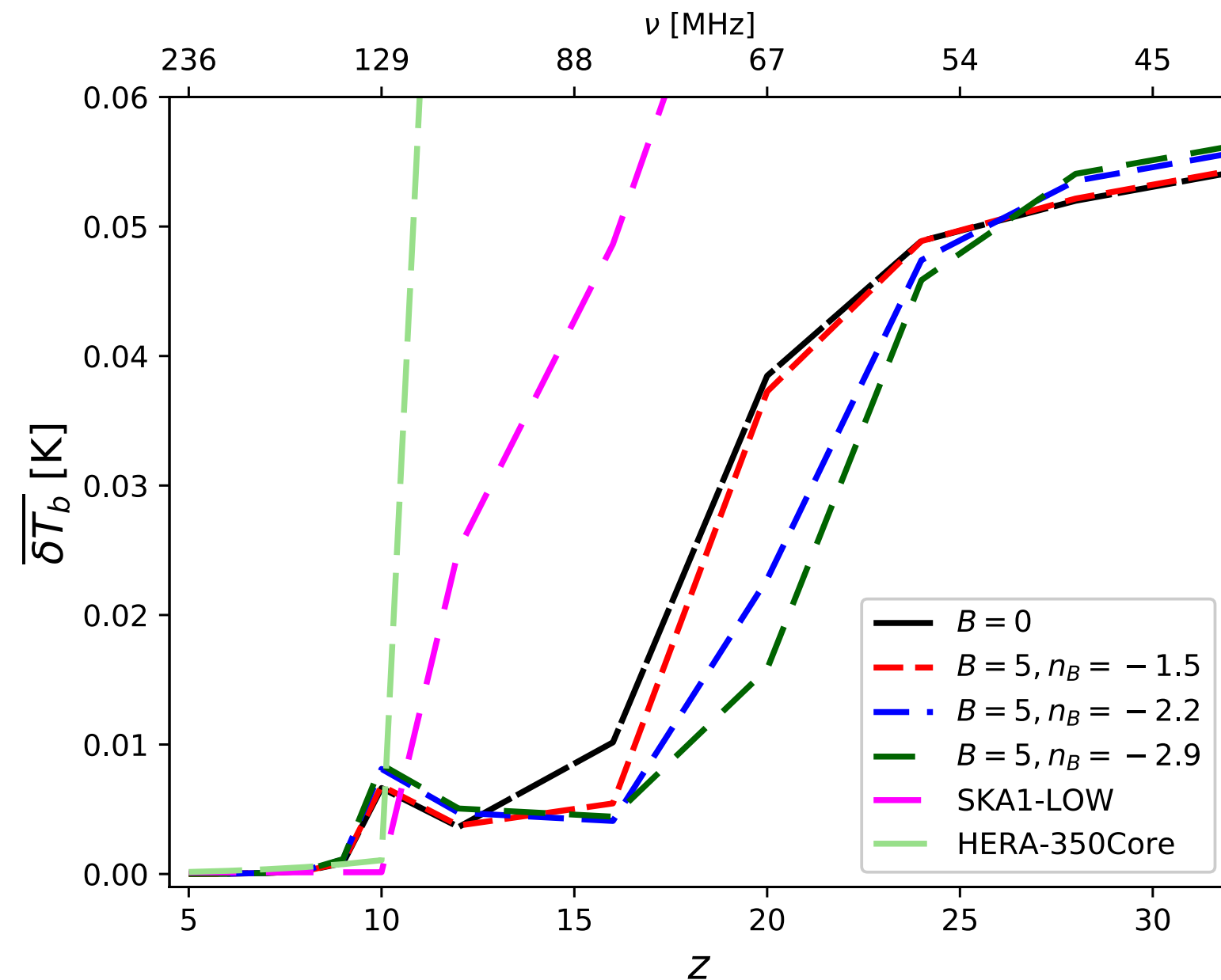
z=32

B=5 nG, nB=-2.9



Observations

- Average 21 cm line signal



KK 2019

SKA1 LOW - the SKA's low-frequency instrument

The Square Kilometre Array (SKA) will be the world's largest radio telescope, revolutionising our understanding of the Universe. The SKA will be built in two phases - SKA1 and SKA2 - starting in 2018, with SKA1 representing a fraction of the full SKA. SKA1 will include two instruments - SKA1 MID and SKA1 LOW - observing the Universe at different frequencies.

Location: Australia

Frequency range: **50 MHz to 350 MHz**

~130,000 antennas spread between **500 stations**

Total collecting area: **0.4km²**

Maximum distance between stations: **65km**

Total raw data output:

- 157 terabytes** per second
- 4.9 zettabytes** per year

Enough to fill up **35,000 DVDs** every second

5x the estimated global internet traffic in 2015 (source: Cisco)

Compared to LOFAR Netherlands, the current best similar instrument in the world

- 25%** better resolution
- 8x** more sensitive
- 135x** the survey speed

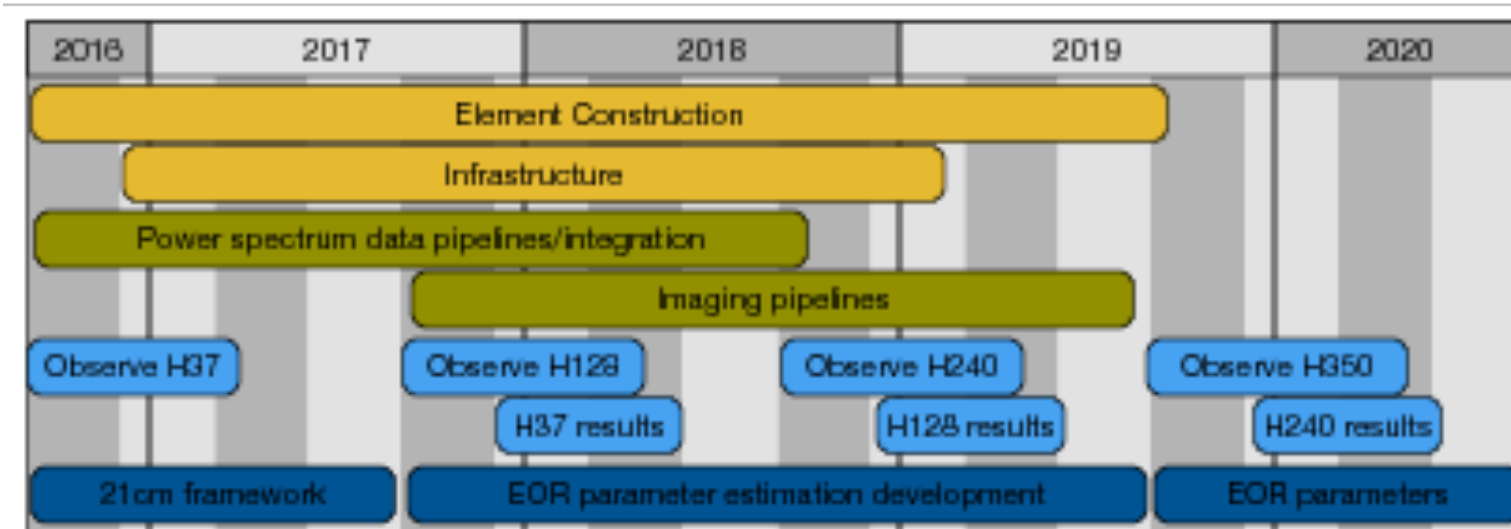
www.skatelescope.org | Square Kilometre Array | @SKA_telescope | The Square Kilometre Array

Observations

- Average 21 cm line signal



Hydrogen Epoch of Reionization Array (HERA)



DeBoer et al. PASP 2017

Table 1

Predicted S/N of 21 cm Experiments for an EoR Model with 50% Ionization at $z = 9.5$, with 1080 hr Observation, Integrated over a Δz of 0.8

Instrument	Collecting Area (m ²)	Foreground Avoidance	Foreground Modeling
PAPER	1,188	0.77 σ	3.04 σ
MWA	3,584	0.31 σ	1.63 σ
LOFAR NL Core	35,762	0.38 σ	5.36 σ
HERA-350	53,878	23.34σ	90.97σ
SKA1 Low Core	416,595	13.4 σ	109.90 σ

Table 2

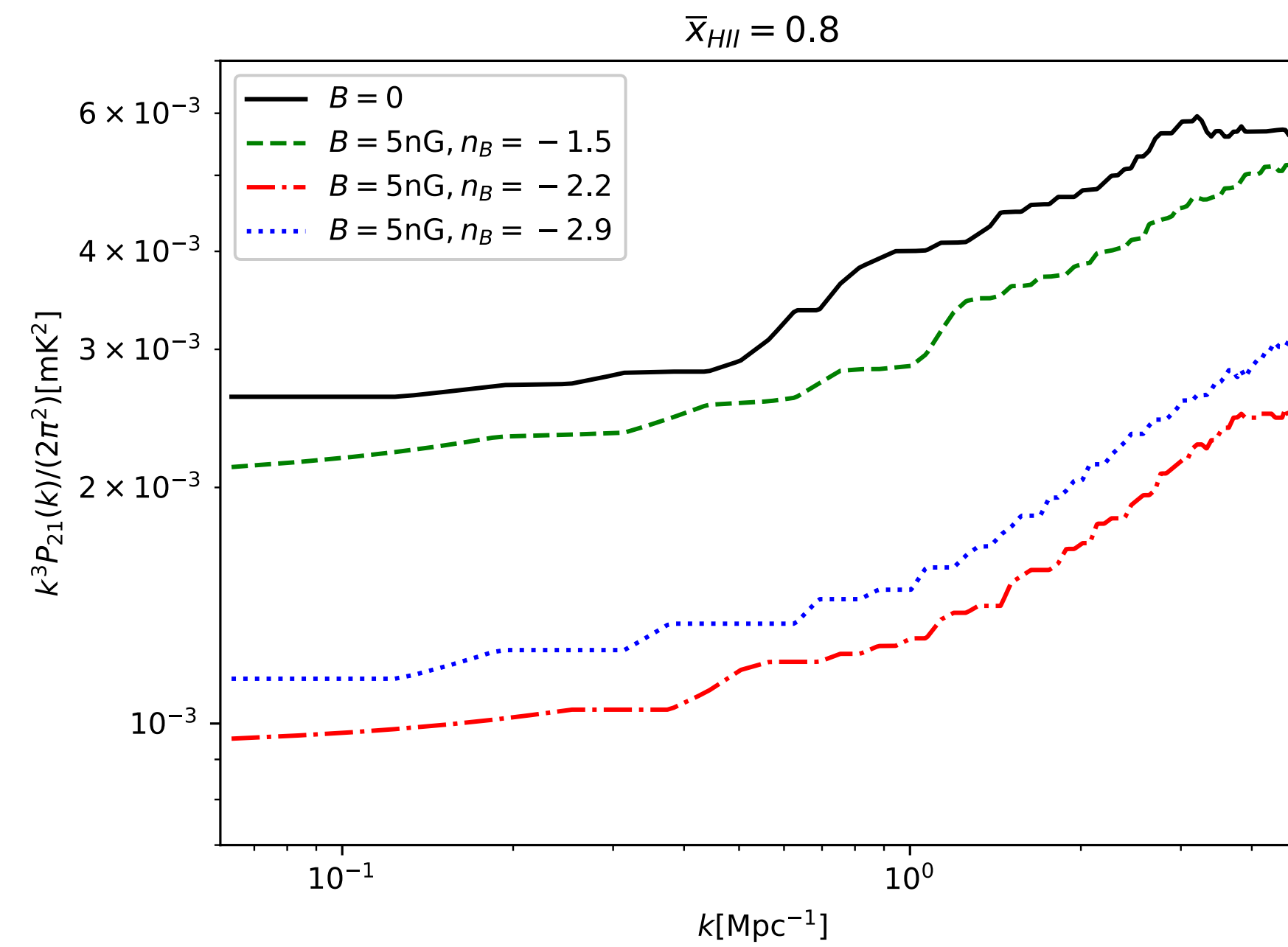
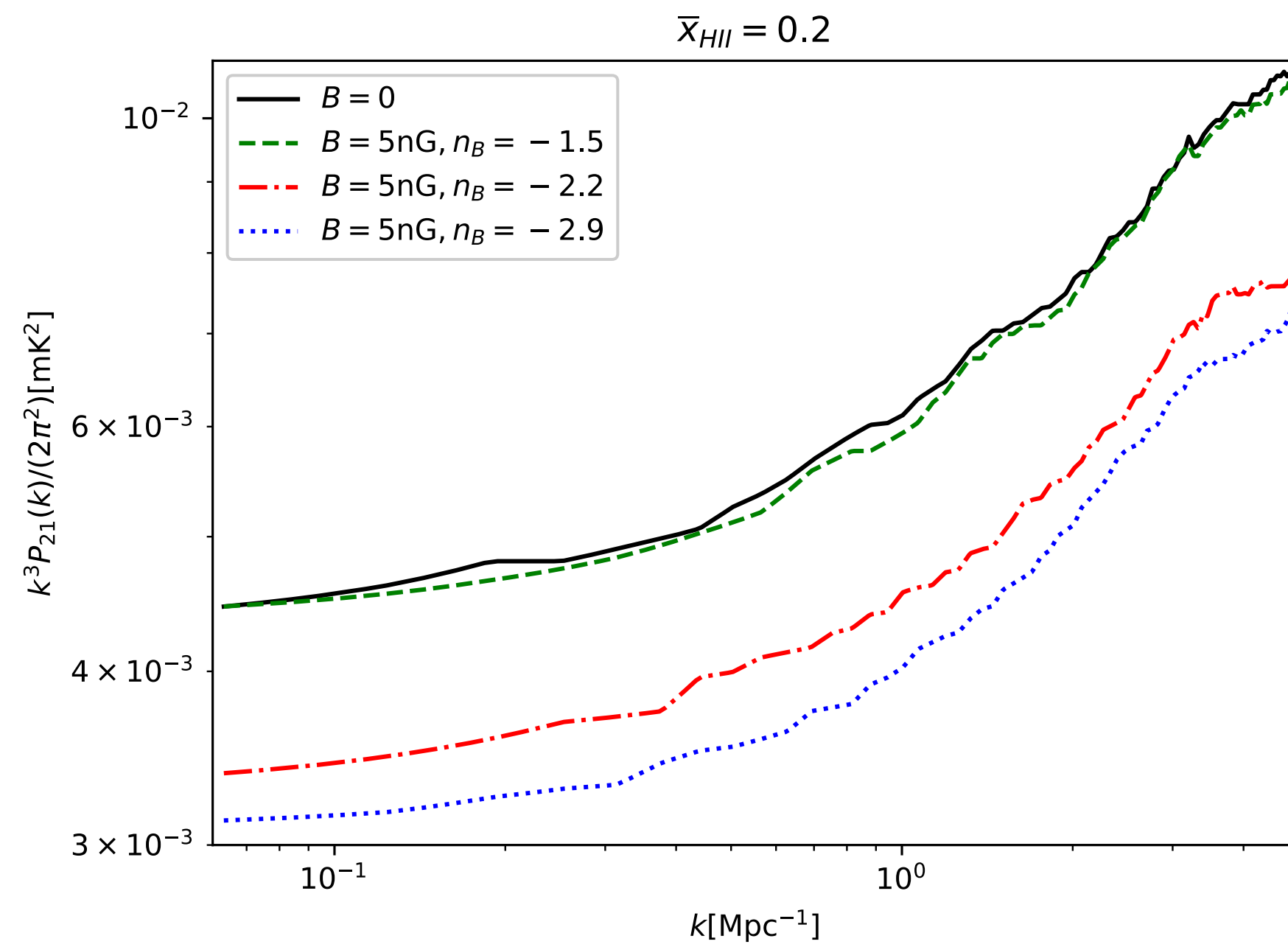
HERA-350 Design Parameters and their Observational Consequences

Instrument Design Specification	Observational Performance
Element Diameter: 14 m	Field of View: 9°
Minimum Baseline: 14.6 m	Largest Scale: 7.8
Maximum Core Baseline: 292 m	Core Synthesized Beam: 25'
Maximum Outrigger Baseline: 876 m	Outrigger Synthesized Beam: 11'
EOR Frequency Band: 100–200 MHz	Redshift Range: 6.1 < z < 13.2
Extended Frequency Range: 50–250 MHz	Redshift Range: 4.7 < z < 27.4
Frequency Resolution: 97.8 kHz	LoS Comoving Resolution: 1.7 Mpc (at $z = 8.5$)
Survey Area: ~1440 deg ²	Comoving Survey Volume: ~150 Gpc ³
$T_{\text{sys}}: 100 + 120(\nu/150 \text{ MHz})^{-2.55} \text{ K}$	Sensitivity after 100 hr: 50 $\mu\text{Jy beam}^{-1}$

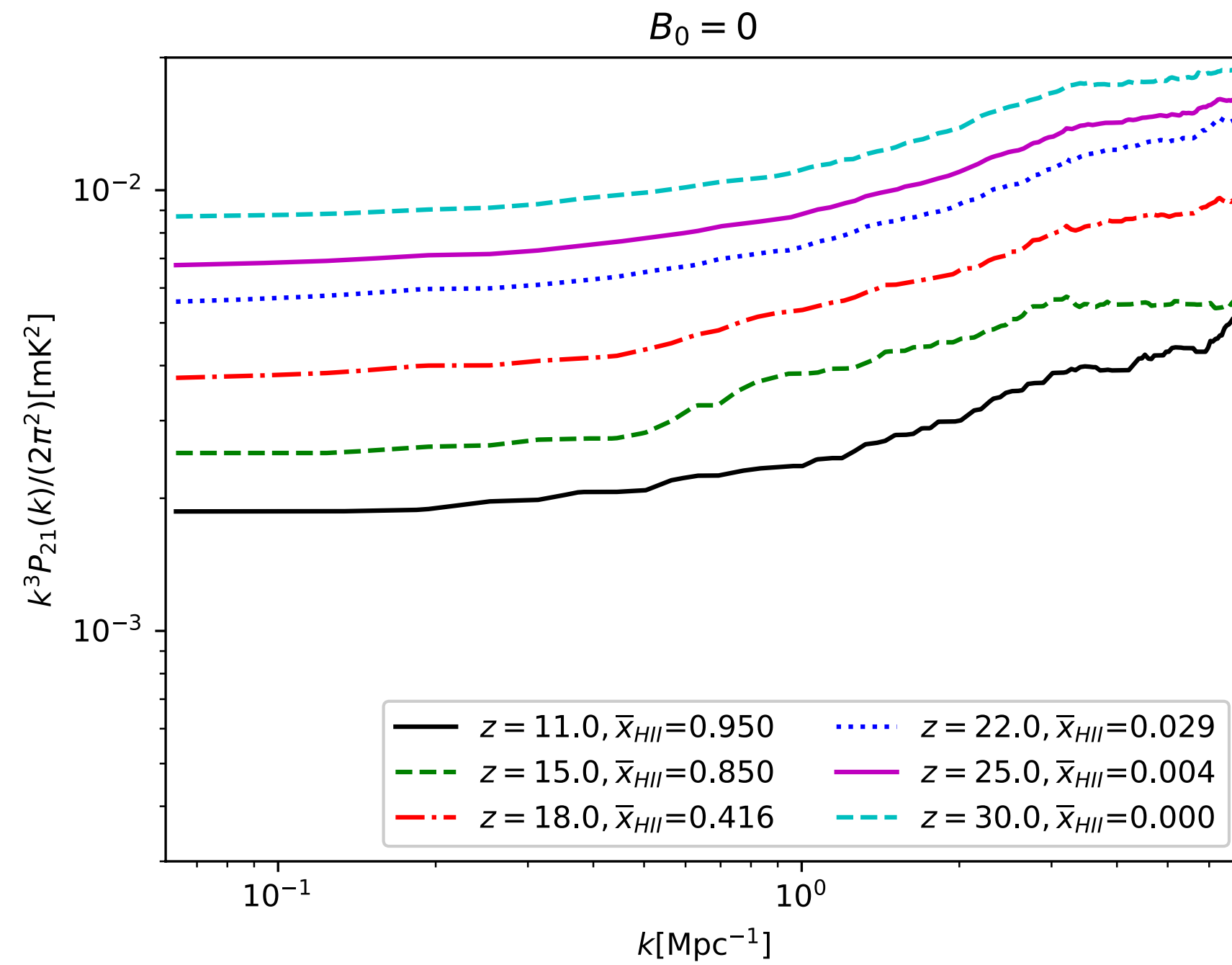
Note. Angular scales computed at 150 MHz.

HERA currently observing in the band 100–200 MHz in the **Karoo Radio Quiet Preserve in South Africa** [DeBoer et al., 2017] at a latitude of -30.73° .

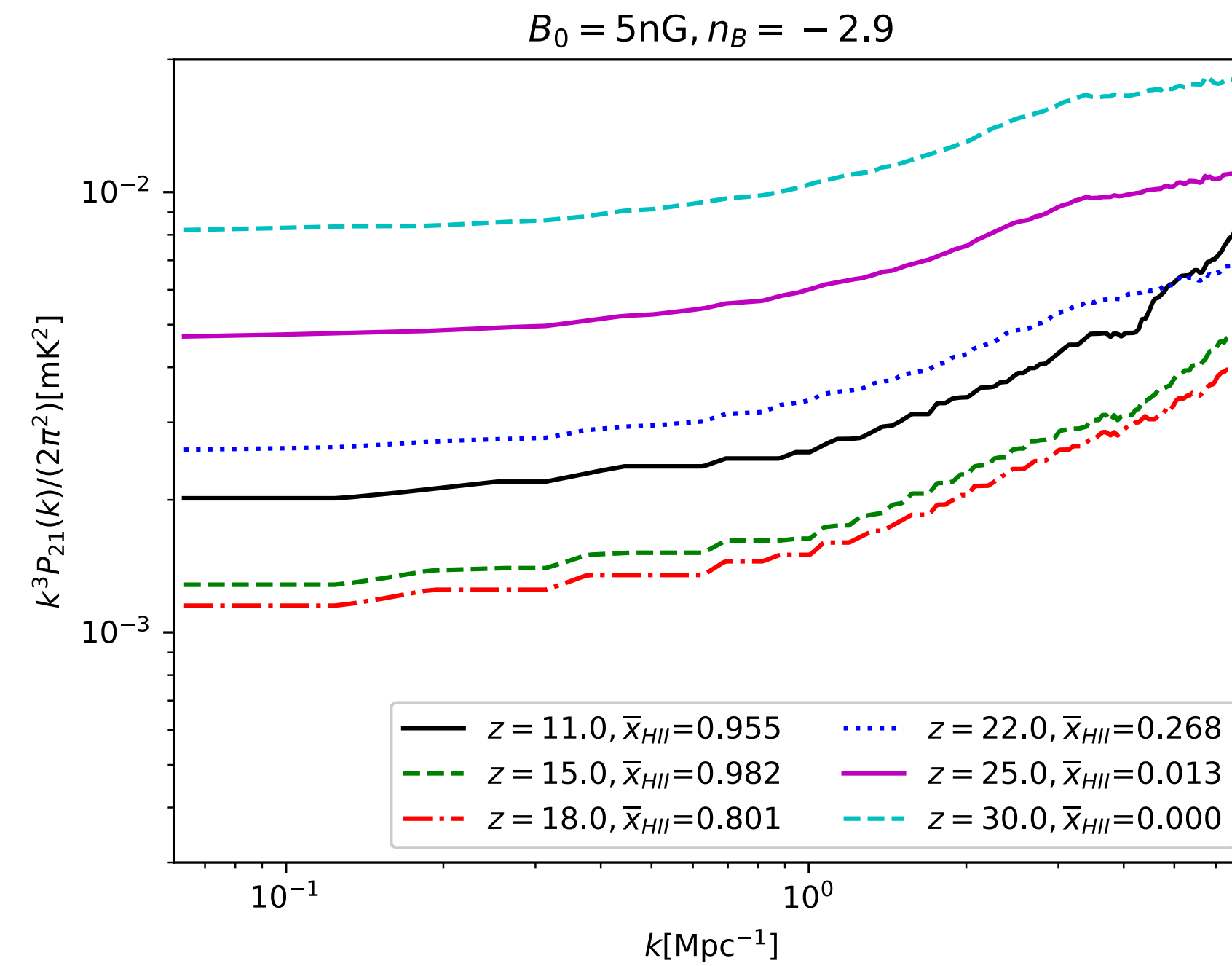
Estimated power spectrum



Estimated power spectrum



B=0



B=5 nG, nB=-2.9

Conclusions

- 21 cm line observations seem to provide a new interesting possibility to constrain primordial magnetic fields.
- 21cm line tomography might be used to constrain magnetic field evolution.